Bubble nucleation in stout beers

W. T. Lee,* J. S. McKechnie, and M. G. Devereux
MACSI, Department of Mathematics and Statistics, University of Limerick, Limerick, Ireland
(Received 2 March 2011; revised manuscript received 10 April 2011; published 31 May 2011)

Bubble nucleation in weakly supersaturated solutions of carbon dioxide—such as champagne, sparkling wines, and carbonated beers—is well understood. Bubbles grow and detach from nucleation sites: gas pockets trapped within hollow cellulose fibers. This mechanism appears not to be active in stout beers that are supersaturated solutions of nitrogen and carbon dioxide. In their canned forms these beers require additional technology (widgets) to release the bubbles which will form the head of the beer. We extend the mathematical model of bubble nucleation in carbonated liquids to the case of two gases and show that this nucleation mechanism is active in stout beers, though substantially slower than in carbonated beers and confirm this by observation. A rough calculation suggests that despite the slowness of the process, applying a coating of hollow porous fibers to the inside of a can or bottle could be a potential replacement for widgets.

DOI: 10.1103/PhysRevE.83.051609 PACS number(s): 47.55.db, 64.60.qj, 82.60.Nh

I. INTRODUCTION

The production of bubbles in weakly supersaturated solutions of carbon dioxide is of great interest to the beverage industry. Such solutions include many soft drinks and beers, as well as sparkling wines and champagne. While it has long been appreciated that spontaneous bubble formation in these liquids is strongly inhibited and thus that bubble formation can only occur at certain nucleation sites [1,2], it is only comparatively recently that the nature of these sites has been fully elucidated. In a series of papers, Liger-Belair and co-workers demonstrated that the most important nucleation sites are pockets of gas trapped in cellulose fibres [3] (an example of type IV nucleation in the classification of Jones *et al.* [2]) and developed a mathematical model of the growth and detachment of these bubbles [4], (a complementary model making slightly different assumptions was developed by Uzel *et al.* [5]).

While most beers are carbonated, there are advantages to using a mixture of nitrogen and carbon dioxide in beers, as is done in a number of stouts. (Hereafter, the term "stout" will be used to refer to a beer containing a mixture of dissolved nitrogen and carbon dioxide.) These advantages include lower acidity in the beer leading to an improved taste, and smaller bubbles giving a creamy mouthfeel and a long lasting head [6,7]. These beers are interesting scientifically because they show interesting fluid dynamical phenomena such as roll waves [8] and sinking bubbles [9]. Also of scientific interest is the technology used to create the head in the canned products.

Pouring a carbonated beer from the can into a glass is enough to generate the head. This is not the case for stouts. Foaming in canned stouts is promoted by a widget: a hollow ball containing pressurized gas. When the can is opened, the widget depressurizes by releasing a gas jet into the beer. The jet breaks up into tiny bubbles which are carried throughout the liquid by the turbulent flow generated by the gas jet and by pouring the beer into a glass. Dissolved gases diffuse from the liquid into the bubbles which rise to the surface of the beer to form the head.

In this paper we extend the mathematical model of bubble formation in carbonated liquids developed by Liger-Belair *et al.* [4] to the case of two dissolved gases and use it to investigate two questions:

(i) Why do stout beers require widgets? Is the bubbling mechanism described by Liger-Belair *et al.* completely inactive in stout beers or merely very slow?

(ii) Could an alternative to the widget be developed by coating part of the inside of the can by hollow fibers?

II. MATHEMATICAL MODEL

In this section we develop a mathematical model of the rate of growth of a gas pocket in a cellulose fiber for the case in which there are two dissolved gases: nitrogen and carbon dioxide. Once a gas pocket reaches a critical size (when it reaches an opening of the fiber) it rapidly forms a bubble outside the fiber, leaving behind the original gas pocket. Since bubble formation and detachment is much faster than the growth of the gas pocket, the rate at which bubbles are nucleated can be deduced from the rate of growth of the gas pocket [4].

The geometry of a gas pocket in a cellulose fiber is shown in Fig. 1. Dissolved gases in the fluid diffuse into the bubble through the walls of the cellulose fiber and through the spherical caps at the ends of the gas pocket. The rate at which this occurs is determined by the surface area, the diffusion constant, and a diffusion length scale. The diffusion constants used to calculate the fluxes of carbon dioxide and nitrogen through the spherical caps are the diffusion constants in free fluid: D_1 and D_2. The relevant diffusion constants for flow through the cellulose walls are $D_{1\perp}$ and $D_{2\perp}$. NMR measurements show that for carbon dioxide $D_{1\perp} \approx 0.2 D_1$ [11]. We assume the same relationship holds between $D_{2\perp}$ and D_2. The diffusion length scale λ was measured experimentally for carbon dioxide [4]; again we assume that this value is also valid for nitrogen diffusion.

*[http://www.ul.ie/wlee]; william.lee@ul.ie

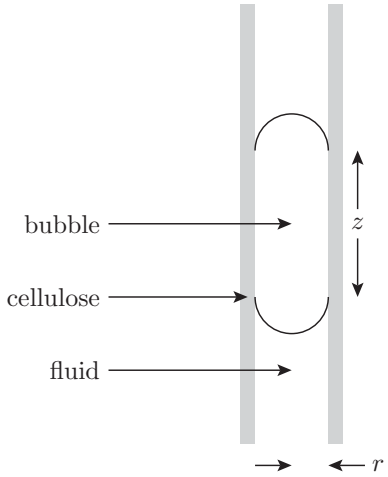

FIG. 1. Geometry of a gas pocket trapped in a cellulose fiber.

In this model the rate of change of the numbers of carbon dioxide (N_1^*) and nitrogen (N_2^*) molecules in the gas pocket are given by

$$\frac{dN_1^*}{dt^*} = 4\pi r^2 D_1 \frac{\Delta c_1}{\lambda} + 2\pi r z D_{1\perp} \frac{\Delta c_1}{\lambda}, \tag{1}$$

$$\frac{dN_2^*}{dt^*} = 4\pi r^2 D_2 \frac{\Delta c_2}{\lambda} + 2\pi r z D_{2\perp} \frac{\Delta c_2}{\lambda}, \tag{2}$$

where asterisks indicate dimensional variables that will be nondimensionalized later.

Using Henry's law, Laplace's law, and the ideal gas equation,

$$\Delta c_1 = H_1 \left(P_1 - \frac{P_B N_1^*}{N_1^* + N_2^*} \right), \tag{3}$$

$$\Delta c_2 = H_2 \left(P_2 - \frac{P_B N_2^*}{N_1^* + N_2^*} \right), \tag{4}$$

$$P_B = P_0 + \frac{2\gamma}{r}, \tag{5}$$

$$z = \frac{\left(N_1^* + N_2^*\right) RT}{\pi r^2 P_B}, \tag{6}$$

where H_1 is the Henry's law coefficient for carbon dioxide, H_2 is the Henry's law coefficient for nitrogen, P_1 is the partial pressure of dissolved carbon dioxide, P_2 is partial pressure of dissolved nitrogen, P_B is the pressure in the gas pocket given by the Laplace law, P_0 is atmospheric pressure, T is temperature, and γ surface tension.

These equations can be nondimensionalized by using the scales,

$$N_{\text{scale}} = \frac{2D_2}{D_{2\perp}} \frac{P_B \pi r^3}{RT} \approx 3.22 \times 10^{-13}\,\text{mol}, \tag{7}$$

$$t_{\text{scale}} = \frac{r P_B \lambda}{2 D_{2\perp} H_2 P_2 RT} \approx 2.73\,\text{s}, \tag{8}$$

to introduce dimensionless variables N_1, N_2, and t (by assumption $D_2/D_{2\perp} = D_1/D_{1\perp}$). The dimensionless equations are

TABLE I. Values of parameters used in this work. r is the radius of the fiber, λ a diffusion length, γ surface tension, T temperature, P_0 ambient pressure. D_i, H_i, and P_i ($i = 1,2$) are the diffusivity, Henry's gas law constant, and partial pressure of dissolved carbon dioxide (subscript 1) and nitrogen (subscript 2). The product $D_i P_i H_i$ controls the rate of diffusion of gas i from solution into the gas pocket.

Parameter	Value	Reference
r	6.00×10^{-6} m	[4]
λ	14.00×10^{-6} m	[4]
γ	47.00×10^{-3} N m^{-1}	[6]
D_1	1.40×10^{-9} m^2 s^{-1}	
D_2	2.00×10^{-9} m^2 s^{-1}	
H_1	3.4×10^{-4} mol m^{-1} N^{-1}	
H_2	6.1×10^{-6} mol m^{-1} N^{-1}	
T	293 K	
P_0	1.00×10^5 Pa	
P_1	0.80×10^5 Pa	[10]
P_2	3.00×10^5 Pa	[10]
$D_1 P_1 H_1$	3.81×10^{-8} mol m^{-1} s^{-1}	
$D_2 P_2 H_2$	3.66×10^{-9} mol m^{-1} s^{-1}	

$$\epsilon \frac{dN_1}{dt} = (1 + N_1 + N_2) \left(1 - \frac{\alpha_1 N_1}{N_1 + N_2} \right), \tag{9}$$

$$\frac{dN_2}{dt} = (1 + N_1 + N_2) \left(1 - \frac{\alpha_2 N_2}{N_1 + N_2} \right). \tag{10}$$

Using values typical of stouts, given in Table I, the dimensionless parameters are

$$\epsilon = \frac{D_2 H_2 P_2}{D_1 H_1 P_1} \approx 0.096, \tag{11}$$

$$\alpha_1 = \frac{P_B}{P_1} \approx 1.45, \tag{12}$$

$$\alpha_2 = \frac{P_B}{P_2} \approx 0.39. \tag{13}$$

III. ASYMPTOTIC SOLUTION

Equations (9) and (10) cannot be solved analytically. They can, however, be solved in two asymptotic limits: $\epsilon \ll 1$ and $N_1 + N_2 \gg 1$. The former limit does not produce particularly accurate results but the analysis of this limit helps us to interpret the results from taking the second asymptotic limit. The results from taking the second asymptotic limit are more accurate but harder to understand intuitively.

A. First asymptotic limit: $\epsilon \ll 1$

Taking the limit in which the small parameter $\epsilon \approx 0.1$ is zero, Eq. (9) becomes an algebraic equation,

$$0 = 1 - \frac{\alpha_1 N_1}{N_1 + N_2}, \tag{14}$$

which can be substituted into Eq. (10),

$$\frac{dN_2}{dt} = \frac{\alpha_1 + \alpha_2 - \alpha_1 \alpha_2}{\alpha_1 - 1} N_2 + \frac{\alpha_1 + \alpha_2 - \alpha_1 \alpha_2}{\alpha_1}. \tag{15}$$

This equation is solved by

$$N_2 = A\exp\left(\frac{t}{\tau}\right) - \frac{\alpha_1+\alpha_2-\alpha_1\alpha_2}{\alpha_1}, \tag{16}$$

where A is a constant of integration and τ a dimensionless time constant describing the time scale of growth of the gas pocket in this approximation,

$$\tau = \frac{\alpha_1 - 1}{\alpha_1+\alpha_2-\alpha_1\alpha_2} \approx 0.35, \tag{17}$$

$$\tau t_{\text{scale}} = 0.954\,\text{s}. \tag{18}$$

The small parameter ϵ used in this analysis is a measure of the relative rates of diffusion of nitrogen and carbon dioxide. As Fick's first law states, the diffusive flux is proportional to the diffusion constant and the concentration gradient, that is, to $D_i P_i H_i/\lambda$ (the Henry's law constant H_i converts the partial pressure P_i into a concentration). For small ϵ we need $D_2P_2H_2 \ll D_1P_1H_1$. As Table I shows, in fact $D_2 > D_1$ and $P_2 > P_1$. Nevertheless ϵ is small because of the very low solubility of nitrogen compared to carbon dioxide ($H_2 \ll H_1$). This means that nitrogen concentrations in solution are much lower than carbon dioxide concentrations (even when the difference in partial pressures is included), and thus that concentration gradients must also be small. Since the concentration gradients of nitrogen are much smaller than the concentration gradients of carbon dioxide, carbon dioxide diffusion is much faster than nitrogen diffusion.

Physically, the $\epsilon \to 0$ approximation corresponds to assuming that diffusion of carbon dioxide is infinitely fast, and thus the partial pressure of carbon dioxide in the gas pocket is always equal to the partial pressure of carbon dioxide in solution. Obviously this approximation is only valid if the partial pressure of carbon dioxide is less than the gas pocket pressure, otherwise Eq. (14) has no physical solutions. Note that this approximation will underestimate τ since it assumes carbon dioxide diffusion is infinitely fast.

B. Second asymptotic limit: $N_1 + N_2 \gg 1$

In the limit $N_1 + N_2 \gg 1$ Eqs. (9) and (10) become

$$\frac{dN_1}{dt} = -\frac{\alpha_1 - 1}{\epsilon}N_1 + \frac{N_2}{\epsilon}, \tag{19}$$

$$\frac{dN_2}{dt} = N_1 + (1-\alpha_2)N_2. \tag{20}$$

TABLE II. Numerical values of the parameters in Eqs. (21) and (22).

Parameter	Value
a_{11}	0.989
a_{12}	0.836
a_{21}	−0.145
a_{22}	0.548
τ_1	0.161
τ_2	0.468
$\tau_1 t_{\text{scale}}$	0.439 *s*
$\tau_2 t_{\text{scale}}$	1.278 *s*

These equations have two independent solutions:

$$N_1 = Aa_{11}\exp\left(-\frac{t}{\tau_1}\right), \quad N_2 = Aa_{21}\exp\left(-\frac{t}{\tau_1}\right), \tag{21}$$

and

$$N_1 = Ba_{12}\exp\left(\frac{t}{\tau_2}\right), \quad N_2 = Ba_{22}\exp\left(\frac{t}{\tau_2}\right), \tag{22}$$

where A and B can be chosen independently to satisfy initial conditions. The numerical values of the other parameters are given in Table II.

The analysis of the $\epsilon \ll 1$ case allows us to interpret these two solutions. The first solution, Eq. (21), decays exponentially with a small time scale. This corresponds to the rapid establishment of the (dynamic) equilibrium concentrations (or partial pressures) of CO_2 and N_2 within the gas pocket (assumed instantaneous in the previous analysis). The second solution, Eq. (22), shows exponential growth with a longer time scale. This describes the steady-state growth of the gas pocket at a fixed concentration ratio of CO_2 to N_2. The time scale of this process describes the time scale of bubble production. This analysis produces a longer estimate of that time scale than the previous analysis. This is because, previously, diffusion of CO_2 was assumed to be instantaneous. As the numerical results described in the next section show, the $\epsilon \ll 1$ limit underestimates the correct time scale, while the $N_1 + N_2 \gg 1$ analysis gives a good estimate.

IV. NUMERICAL SOLUTION

A full solution of the dimensionless equations can be obtained by numerical integration. A fourth-order Runge-Kutta scheme with a time step of 10^{-3} was used to solve

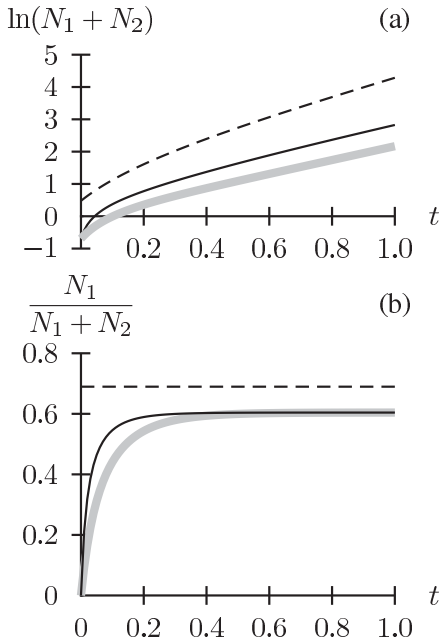

FIG. 2. Results of the numerical solution of Eqs. (9) and (10). The black line shows the numerical solution, the gray line shows the $N_1 + N_2 \gg 1$ limit, and the dashed black line shows the $\epsilon \ll 1$ limit. (a) Rate of growth of the gas pocket. (b) Evolution of the concentration of CO_2 in the gas pocket.

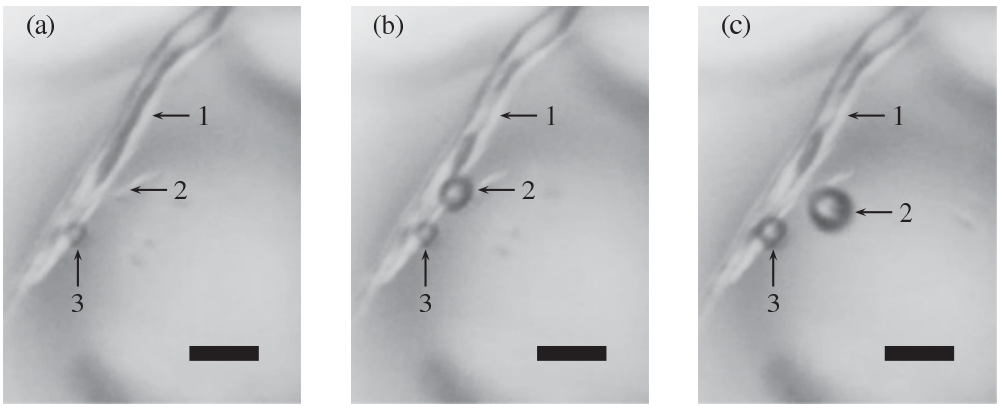

FIG. 3. Bubble nucleation in stout from a cellulose fiber taken from a coffee filter. The scale bar is 50 μm in each figure. The arrows show (1) a gas pocket in the fiber which nucleates a bubble; (2) the bubble fed by gas from pocket 1; (3) a bubble nucleated on the outside of the fiber. (a) The air pocket (1) has reached maximum size. (b) The air pocket (1) has created bubble (2). (c) Bubble (2) has visibly detached from the fiber, air pocket (1) is starting to refill with gas. (a), (b), and (c) are frames from a movie. (b) is 80 ms after (a), (c) is 520 ms after (a).

Eqs. (9) and (10) with initial conditions $N_1 = 0$, $N_2 = 0.5$. The differential equations were solved over the interval $0 < t < 10$. The result for $N = N_1 + N_2$ for $5 < t < 10$ were fitted to an exponential curve giving a dimensionless bubble growth time scale of $\tau = 0.47$ corresponding to a dimensional time scale of $\tau t_{\text{scale}} = 1.28$ s, in agreement with that predicted from the analysis of the $N_1 + N_2 \gg 1$ case. This can be compared with the value for carbonated liquids at the same total pressure: 0.079 s. Figure 2 shows the results of the numerical simulations over the interval $0 < t < 1$.

In conclusion, these analytic and numerical results suggest that the mechanism of bubble formation described by Liger-Belair *et al.* is potentially active in stout beers but acts much more slowly than in carbonated drinks.

V. EXPERIMENTAL CONFIRMATION

To confirm experimentally that cellulose fibers could nucleate bubbles in stout beer, we observed a canned draught stout in contact with cellulose fibers (taken from a coffee filter). Before opening the can, we made a small hole in the can to slowly degas the widget. This prevented it from foaming, which would have removed the dissolved gases from solution. Using a microscope we observed that bubbles were indeed nucleated from the cellulose fibers but at a slow rate, compared to the rate of bubble nucleation in carbonated liquids. Figure 3 shows bubbles nucleated by a gas pocket: The three parts of Fig. 3 are frames taken from a movie.

The frames of the movie can be used to construct a picture of the growth of the gas pocket. Figure 4 illustrates the steps of the process. Two hundred frames (from the same movie of the bubbling process used for Fig. 3), corresponding to 8 s were extracted from the movie [Fig. 4(a)] and rotated so that the fiber shown in Fig. 3 was vertical [Fig. 4(b)]. From each frame a strip of 1×175 pixels, passing through the center of the fibre, was extracted and those strips placed side by side [Fig. 4(c)] to construct a new figure: Fig. 5. This figure shows the evolution of the gas pocket: its slow growth (as predicted by the model) and then its rapid loss of gas to form an external bubble (as assumed by the model). In the figure, the nucleation period is about 3.5 s, roughly three times that predicted by the model. The reason for this is the figure was taken some time after the stout had come into contact with the fibers (in

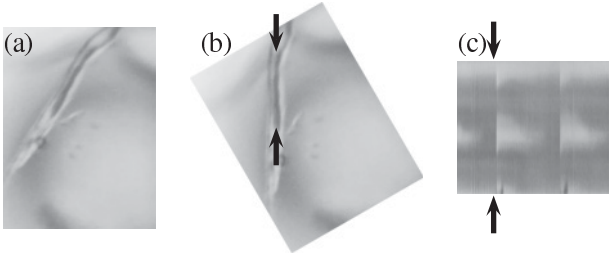

FIG. 4. Process used to construct Fig. 5. The figure was constructed from 200 frames of a movie. (a) One of the frames from the movie. (b) Each frame was rotated to make the fiber vertical, and a strip of pixels (indicated by arrows) extracted. (c) The strips of pixels from each frame of the movie were laid side by side to make Fig. 5.

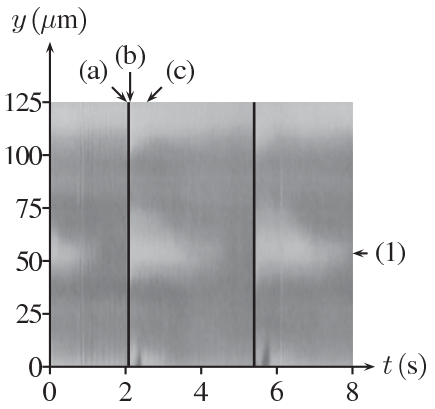

FIG. 5. Growth of the gas pocket. The construction of the figure is described in the main text and illustrated in Fig. 4. This figure shows the growth of the gas pocket within the cellulose fiber shown in Fig. 3. As in Fig. 3 dark colors correspond to gas and light colors to liquid. The columns of pixels from the frames corresponding to parts (a), (b), and (c) of Fig. 3 are indicated. The location of the gas pocket indicated by a (1) in Fig. 3 is shown. Vertical lines indicate the times at which bubbles are created by the fiber.

TABLE III. Values of the parameter ϵ when nitrogen is replaced by other gases.

Gas	D (10^{-9} m^2 s^{-1})	H (10^{-5} mol m^{-1} N^{-1})	ϵ
Hydrogen	5.11	0.78	0.31
Oxygen	2.42	1.26	0.24
Methane	1.84	1.32	0.19

order to obtain clearer figures), so that the gas concentrations were lower than their initial values, due to losses through the free surface and bubbling. Earlier, bubble formation at rates comparable to those calculated from the model above was observed.

VI. WIDGET ALTERNATIVES

The model developed above allows us to investigate the feasibility of an alternative foaming strategy for stout beers in cans and bottles in which a coating of hydrophobic fibers on the inside of the can is used to promote foaming. A typical pouring time for a stout beer is 30 s. In this time about 10^8 postcritical nuclei must be released. A single fiber produces one bubble every 1.28 s. Therefore about 4.3×10^6 fibers are needed. If each fiber occupies a surface of area λ^2 then the total area that must be occupied by fibers is 8.3×10^{-4} m^2 equivalent to a square with edge length 2.9 cm. This indicates that such an approach may be possible.

VII. CONCLUSIONS

A model of bubble formation in carbonated liquids has been extended to the case of liquids containing both dissolved nitrogen and carbon dioxide. Taking values typical of stout beers shows that bubble formation by this mechanism does occur but at a substantially slower rate. This is consistent with the observation that widgets are needed to promote foaming in canned stouts. This is due to two effects, described by the parameters α_1 and ϵ in the model. First, the pressure of the more soluble gas is lower than the pressure in the gas pocket: $\alpha_1 > 1$. This means that the more soluble gas cannot create bubbles on its own. If $\alpha_1 < 1$ then bubbles would be created containing mostly carbon dioxide and trace amounts of nitrogen, and the stout beer would be indistinguishable from a carbonated beer. Second, as described by the parameter ϵ, diffusion of the less soluble gas is much slower than diffusion of the more soluble gas. As noted previously, by Fick's first law, rates of diffusion are proportional to the diffusion constant and the concentration gradient of dissolved gases [i.e., to the product $D_i P_i H_i/\lambda$ $(i = 1,2)$]. While the diffusion constant D_2 and the partial pressure of nitrogen P_2 are higher than those of carbon dioxide and by assumption λ is the same for both gases, the Henry's law coefficient H_2 which converts the partial pressure into a concentration is about 50 times smaller than that of carbon dioxide, this ensures that $\epsilon \ll 1$. The analysis is also relevant if nitrogen is replaced by other low solubility gases, although these might be of less interest to the beverage industry. For instance, as shown in Table III, if nitrogen was replaced by hydrogen, oxygen, or methane, ϵ would become 0.31, 0.24, or 0.19, respectively. Finally, the possibility of replacing widgets with an array of hollow fiber nucleation sites was investigated and shown to be potentially feasible.

ACKNOWLEDGMENTS

We acknowledge support of the Mathematics Applications Consortium for Science and Industry [http://www.macsi.ul.ie] funded by the Science Foundation Ireland Mathematics Initiative Grant No. 06/MI/005. M.G.D. acknowledges funding from the Irish Research Council for Science, Engineering and Technology (IRCSET).

[1] J. Walker, Sci. Am. **245**, 172 (1981).
[2] S. F. Jones, G. M. Evans, and K. P. Galvin, Adv. Colloid Interface Sci. **80**, 51 (1999).
[3] G. Liger-Belair, M. Vignes-Adler, C. Voisin, B. Robillard, and P. Jeandet, Langmuir **18**, 1294 (2002).
[4] G. Liger-Belair, C. Voisin, and P. Jeandet, J. Phys. Chem. B **109**, 14573 (2005).
[5] S. Uzel, M. A. Chappell, and S. J. Payne, J. Phys. Chem. B **110**, 7579 (2006).
[6] C. W. Bamforth, J. Inst. Brew. **110**, 259 (2004).
[7] M. Denny, in *Froth!: The Science of Beer* (The Johns Hopkins University Press, Baltimore, 2009), pp. 129–131.
[8] M. Robinson, A. C. Fowler, A. J. Alexander, and S. B. G. O'Brien, Phys. Fluids **20**, 067101 (2008).
[9] Y. Zhang and Z. Xu, Elements **4**, 47 (2008).
[10] O. A. Power, W. T. Lee, A. C. Fowler, P. J. Dellar, L. W. Schwartz, S. Lukaschuk, G. Lessells, A. F. Hegarty, M. O'Sullivan, and Y. Liu, in *The Initiation of Guinness*, *Proceedings of the Seventieth European Study Group with Industry*, edited by S. B. G. O'Brien, M. O'Sullivan, P. Hanrahan, W. T. Lee, J. Mason, J. Charpin, M. Robinson, and A. Korobeinikov (University of Limerick, Limerick, 2009), pp. 141–182.
[11] G. Liger-Belair, D. Topgaard, C. Voisin, and P. Jeandet, Langmuir **20**, 4132 (2004).